Exploratory Correlation of The Human Structural Connectome with Non-MRI Variables in Alzheimer's Disease

Iman Aganj, [a,b,*] Jocelyn Mora, [a] Aina Frau-Pascual, [a,b] Bruce Fischl, [a,b]

for the Alzheimer's Disease Neuroimaging Initiative

{iaganj, bfischl}@mgh.harvard.edu , {joceymora, ainafp}@gmail.com

[a] Athinoula A. Martinos Center for Biomedical Imaging, Radiology Department, Massachusetts General Hospital, 149 13th St., Suite 2301, Boston, MA 02129, USA

[b] Radiology Department, Harvard Medical School, 25 Shattuck St., Boston, MA 02115, USA

[*] Corresponding author:

Iman Aganj

Email: iaganj@mgh.haravrd.edu
Telephone: +1 (617) 643-7791
Web: https://iman.mgh.harvard.edu
Address: 149, 13th St., Suite 2301, Boston, MA 02129, USA

[†] Data used in the preparation of this article were obtained from the Alzheimer's Disease Neuroimaging Initiative (ADNI) database (adni.loni.usc.edu). As such, the investigators within the ADNI contributed to the design and implementation of ADNI and/or provided data but did not participate in the analysis or writing of this report. A complete listing of ADNI investigators can be found at:
http://adni.loni.usc.edu/wp-content/uploads/how_to_apply/ADNI_Acknowledgement_List.pdf

ABSTRACT

INTRODUCTION: Discovery of the associations between brain structural connectivity and clinical and demographic variables can help to better understand the vulnerability and resilience of the brain architecture to neurodegenerative diseases and to discover biomarkers.

METHODS: We used four diffusion-MRI databases, three related to Alzheimer's disease, to exploratorily correlate structural connections between 85 brain regions with non-MRI variables, while stringently correcting the significance values for multiple testing and ruling out spurious correlations via careful visual inspection. We repeated the analysis with brain connectivity augmented with multi-synaptic neural pathways.

RESULTS: We found 34 and 37 significant relationships with direct and augmented connectivity, respectively, which were generally stronger for the latter. Age was consistently linked to decreased connectivity, and healthier clinical scores were generally linked to increased connectivity.

DISCUSSION: Our findings help to elucidate which structural brain networks are affected in Alzheimer's disease and aging and highlight the importance of including indirect connections.

Keywords: Structural brain connectivity, human connectome, multi-synaptic neural pathways, diffusion MRI, Alzheimer's disease, dementia, aging.

1. Introduction

Normal aging, as well as debilitating neurodegenerative diseases such as Alzheimer's disease (AD), affect not only individual brain regions, but also connectivity between them [1, 2]. Focus on brain regions, but not interregional connectivity, may have hindered progress in understanding and treating diseases such as AD that are characterized as disconnection syndromes [3]. Mapping the complex brain networks through which information flows – i.e., the human *connectome* [4] – can help to better understand the vulnerability and resilience of these networks to the effects of AD, potentially leading to the discovery of diagnostically and therapeutically important connectomic biomarkers. Analysis of structural brain networks, by means of noninvasive diffusion-weighted magnetic resonance imaging (dMRI), has proved valuable in revealing the structural basis of dysfunction in mild cognitive impairment (MCI) and AD, demonstrating changes distinct from those with healthy aging [5-9].

Brain connectivity is often represented as a graph adjacency matrix of connection strengths between the brain regions of interest (ROIs), with its number of elements (graph edges) growing quadratically with respect to the number of ROIs (graph nodes). In population connectomic studies, it is often desired to find links between brain connectivity and non-MRI (clinical and/or demographic) variables. Such a study typically has sufficient statistical power to test pre-hypothesized relationships involving specific brain connections and variables. In contrast, an exploratory investigation to *discover* previously unknown relationships would require correlating the connectivity strength of every brain ROI pair with every available variable, amounting to hundreds of thousands (sometimes millions) of tests. In that scenario, the correction for multiple comparisons would make the study statistically less powerful and consequently less desirable to conduct. Alternatively, one could reduce the number of tests considerably by focusing on network summary features [10] rather than brain connections, which would inform about how the variables relate to the network as a whole [7, 11] but not to individual brain connections.

Structural connectivity between two brain regions is commonly defined based on the dMRI tractography-derived [12, 13] streamlines between them. The direct fiber bundle connecting two brain areas is expected to be the major signal carrier between them; however, *multi-synaptic* neural pathways (those mediated through other regions) also provide connectivity [14, 15]. We have previously developed computational methods to augment direct structural connectivity graphs with indirect connections [16] as well as quantify brain structural connectivity while accounting for indirect pathways [17], and have shown the importance of these pathways in predicting functional connectivity [17] and deriving connectomic biomarkers for MCI and AD [18].

Here, we take an exploratory approach to discovering relationships that individual structural connections in the brain may have with clinical and demographic variables. We use anatomical and diffusion MR images along with non-MRI data from four public databases (three of which are related to AD) to find links between brain connections – both direct and augmented – and non-

MRI variables that remain significant after stringent correction for multiple testing and visual inspection.

We describe our processing and analysis methods in Section 2, report our results in Section 3, discuss them in Section 4, and conclude the paper in Section 5.

2. Methods

2.1. Datasets

We used the following four public dMRI databases. The number of subjects indicates the subset of subjects that were processed and included in our analysis, and the number of non-MRI variables indicates variables that were available for at least some of the included subjects.

- The second phase of the *Alzheimer's Disease Neuroimaging Initiative (**ADNI-2**)* [19]: 217 subjects (from cognitively normal to AD), 47 non-MRI variables from the `ADNIMERGE` table (demographics, CSF markers, dementia/cognitive exam scores, PET, ApoE4, diagnosis, …).
- The third release in the *Open Access Series of Imaging Studies (**OASIS-3**)* [20]: 771 subjects (from cognitively normal to AD), 23 non-MRI variables (demographics, dementia/cognitive exam scores, ApoE, …).
- The *Pre-symptomatic Evaluation of Experimental or Novel Treatments for Alzheimer's Disease (**PREVENT-AD**)* [21]: 340 cognitively unimpaired older individuals with a parental or multiple-sibling history of AD, 199 non-MRI variables (demographics, medical history, vitals, CSF markers, dementia/cognitive exam sub-scores, genetics, lab results, auditory/olfactory processing, …).
- The WashU-UMN *Human Connectome Project (**HCP**)* [22]: 617 healthy young adults, 488 non-MRI variables (demographics, medical history, family history, dementia/cognitive exam scores, personality/emotion tests, motor/sensory tests, task performance, …).

2.2. Data processing

Anatomical MR images of the databases were processed with FreeSurfer [23]. All time points of PREVENT-AD were also more robustly processed using the FreeSurfer longitudinal pipeline [24]. Nevertheless, for all databases, we included each subject only once, i.e. the earliest visit containing dMRI (frequently the baseline), in order to keep our analyzed data points independent and our study cross-sectional. We then ran the FreeSurfer dMRI processing pipeline, which also includes

commands from the FMRIB Software Library (FSL) [25], and propagated the 85 automatically segmented cortical and subcortical regions from the structural to the diffusion space using boundary-based image registration [26].

Next, we used our public toolbox (www.nitrc.org/projects/csaodf-hough) to: 1) reconstruct the diffusion orientation distribution function in constant solid angle [27], 2) run Hough-transform global probabilistic tractography [13] to generate an optimal (highest-score) streamline passing through each of the 10,000 seed points per subject, 3) compute a symmetric structural connectivity matrix (with positive elements) for each subject by summing the tracts passing through each pair of ROIs weighted by the tract score (hence an emphasis on streamlines best aligned with the dMRI-derived fiber orientations as well as fiber tracts with the highest white-matter integrity), and 4) augment the raw matrices with indirect connections (see Section 2.3) [16]. We transformed the connectivity value c (each element in the raw or augmented connectivity matrix) as $c \leftarrow 1 - \exp(-c/\bar{c})$, where $\bar{c}$ is the cross-subject average of c, thereby confining the connectivity values to the range [0,1).

2.3. Augmentation of structural connectivity with indirect connections

Strong functional connectivity between brain regions are commonly observed between regions with no *direct* structural connection [14, 28-34]. Some variance in functional connectivity unexplained by direct connections can be accounted for by *indirect* structural connections [14, 15, 17], implying that the network nature of the brain makes the interaction between two brain areas sensitive to influences from other remote areas [29].

We have previously developed a method to augment a tractography-generated structural connectivity matrix with indirect connections via the mathematics of circuits laws [16], thereby producing a new matrix that additionally reflects multi-synaptic pathways. This approach is based on the intuition that total connectivity for multiple direct connections is expectedly their sum if they are parallel, or smaller than each connection if they are in series (as total connectivity is presumably bottlenecked by the weakest link along the way). These conditions are accommodated by modeling the brain similarly to a resistive electrical circuit, where a resistor represents each direct connection, with its conductance (inverse of resistance) being the tractography-measured strength of the connection [16, 35]. Total (augmented) connectivity is then calculated via Kirchhoff's laws as the overall conductance among regions, using graph Laplacian methods.

2.4. Analysis

We used the cross-sectional data of each database to independently test if there is a statistically significant relationship between each non-MRI (clinical or demographic) variable and the

computed structural brain connection between each ROI pair. To deal with data source heterogeneity, we analyzed the databases and report their results separately. The homogeneity within each database is expected to lead to findings that would be strengthened if they independently replicated in several databases.

If a non-MRI variable had categorical (rather than numeric) values, we converted it to numeric by assigning a natural number to each category, while making our best effort to sort the categories (if more than two) in a monotonic order; for instance, for Baseline Diagnosis in ADNI-2, we assigned: Control Normal → 1, Significant Memory Concern → 2, Early MCI → 3, Late MCI → 4, and AD → 5. We then computed the Pearson correlation coefficient (r), along with its significance (p) value, between each variable and each connection. The p-values were corrected for multiple comparisons via the conservative Bonferroni method (p_b); i.e., they were multiplied by the number of (undirected) connections, #ROIs×(#ROIs-1)÷2 = 85×84÷2 = 3570, as well as by the number of studied variables (see Section 2.1). Since the quantified structural connectivity, which is the score-weighted number of streamlines passing through a pair of ROIs, is affected by the tract length, we controlled for the extraneous variable of intracranial volume (ICV) by computing the *partial* correlation instead. For robustness of the correlation [36], we removed connectivity values that were marginal outliers from the correlation analysis by excluding any element in the connectivity matrix of a subject (but not the subject's entire matrix) that was larger than 0.9 (recall the range [0,1) of values). This was principally because we deemed a connectivity value with a large deviation from the population mean less reliable, since such a deviation indicated an increased likelihood of lower image quality or a data-processing issue. Therefore, slightly different numbers of subjects contributed to the correlation analysis of different brain connections.

For each variable, we selected the connection most significantly correlating with it, i.e. with the lowest p_b-value. If p_b was smaller than the threshold α=0.05, then we scatter-plotted the connection strength with respect to the variable and visually inspected it to ensure the significant Pearson correlation was real and not spurious due to some outliers, thus avoiding situations with most data points clustered together with no obvious relationship [36]. The correlations surviving the Bonferroni correction and passing the visual inspection are reported as follows.

3. Results

We correlated 3570 brain structural connections with 47, 23, 199, and 488 non-MRI variables for each of the ADNI-2, OASIS-3, PREVENT-AD, and HCP databases, respectively, while controlling for the ICV. Out of those variables, 15, 20, 32, and 82, respectively, were found to have significant Pearson correlation ($p_b < 0.05$) with raw connections, and 20, 17, 1, and 0 variables, respectively, had significant correlation with augmented connections. After visual inspection to remove spurious correlations, variables with significant correlation with raw connectivity were reduced to 15, 16, 3, and 2, respectively, whereas the variables significantly

correlated with augmented connectivity remained unchanged. The findings are detailed in Tables 1 through 4 for the four databases. The right column indicates the total number (out of 3570) of connections reaching Bonferroni-level significance for a given variable. Note that we included a single Uniform Data Set (UDS) variable in Table 2, as different UDS assessment scores in OASIS-3's General Demographics table appeared to have identical values.

Controlling for ICV had several effects on the results, e.g., it made the correlation of brain connectivity with *ECog SP – Memory* in ADNI-2 significant (see

Table 1). Without separating the effects of ICV, conversely, we would observe significant negative correlations of brain connectivity with *grip strength* and the *maximum number of drinks consumed in a single day* in HCP. The confounding effect of ICV was especially drastic on the correlation with sex. Significant correlation of connectivity (of the most related brain connection) with the *male sex* was:

- initially not found in ADNI-2 but appeared as positive by including ICV as a covariate,
- negative in OASIS-3 regardless of controlling for ICV (but stronger without),
- initially positive in PREVENT-AD but disappeared after including ICV as a covariate,
- initially negative in HCP but disappeared after including ICV as a covariate.

Next, we focused on three representative variables of age, MMSE, and CDR (sum of boxes). Among all the augmented brain connections that were significantly correlated with age (after Bonferroni correction) consistently in ADNI-2, OASIS-3, and PREVENT-AD, the connection between the right superior frontal cortex and the left hippocampus was most significant (in terms of the geometric mean of the *p*-values across databases). Similarly, for both MMSE and CDR, the augmented connection between the right superior frontal cortex and the right hippocampus had the most significant correlation consistently in ADNI-2 and OASIS-3. These relationships are plotted in Figure 1 for all three variables.

Table 1: Significant correlations of non-MRI variables with brain connectivity in ADNI-2.

Non-MRI variable	Most correlated brain structural connection	# Sig. Conn
Baseline Diagnosis	L. Lingual cortex – L. Entorhinal cortex *Augmented*, r = -0.41, p_b = 0.0005	79
Age	L. Ventral diencephalon – L. Hippocampus *Raw*, r = -0.42, p_b = 0.0002	7
	R. Superior frontal cortex – L. Hippocampus *Augmented*, r = -0.47, $p_b = 7 \times 10^{-7}$	67
Sex	R. Putamen – Brainstem *Raw*, r = 0.36 (with the male sex), p_b = 0.04	2
FDG-PET *Mean of angular, temporal, and posterior cingulate*	R. Fusiform cortex – R. Hippocampus *Raw*, r = 0.43, p_b = 0.0001	3
	R. Precuneus cortex – R. Hippocampus *Augmented*, r = 0.46, $p_b = 4 \times 10^{-6}$	67
AV45 PET (binding to β-amyloid) *Mean of whole cerebellum*	R. Precuneus cortex – R. Hippocampus *Augmented*, r = -0.43, $p_b = 8 \times 10^{-5}$	45
Clinical Dementia Rating (CDR) *Sum of boxes*	R. Fusiform cortex – R. Hippocampus *Raw*, r = -0.38, p_b = 0.007	3
	R. Entorhinal cortex – L. Pallidum *Augmented*, r = -0.43, $p_b = 6 \times 10^{-5}$	135
AD Assessment Scale (ADAS) *11 items*	R. Fusiform cortex – R. Hippocampus *Raw*, r = -0.37, p_b =0.03	2
	R. Precuneus cortex – R. Hippocampus *Augmented*, r = -0.43, p_b = 0.0001	45
AD Assessment Scale (ADAS) *13 items*	R. Hippocampus – R. Fusiform cortex *Raw*, r = -0.39, p_b = 0.005	2
	R. Precuneus cortex – R. Hippocampus *Augmented*, r = -0.44, $p_b = 4 \times 10^{-5}$	86
AD Assessment Scale (ADAS) *Delayed Word Recall*	R. Ventral diencephalon – R. Hippocampus *Raw*, r = -0.38, p_b = 0.01	4
	R. Caudal anterior cingulate cortex – L. Entorhinal cortex *Augmented*, r = -0.40, p_b = 0.0008	42
Mini-Mental State Examination (MMSE)	R. Entorhinal cortex – R. Hippocampus *Raw*, r = 0.37, p_b = 0.02	2
	R. Entorhinal cortex – L. Amygdala *Augmented*, r = 0.42, p_b = 0.0003	75
Rey Auditory Verbal Learning Test (RAVLT) Immediate *Sum of 5 trials*	R. Entorhinal cortex – R. Hippocampus *Raw*, r = 0.39, p_b = 0.006	1
	R. Isthmus cingulate cortex – L. Entorhinal cortex *Augmented*, r = 0.41, p_b = 0.0005	70
Functional Assessment Questionnaire (FAQ)	R. Fusiform cortex – R. Hippocampus *Raw*, r = -0.38, p_b = 0.01	2
	R. Rostral middle frontal cortex – R. Hippocampus *Augmented*, r = -0.46, $p_b = 10^{-6}$	142

Montreal Cognitive Assessment (MoCA)	L. Middle temporal cortex – L. Hippocampus *Raw*, $r = 0.39$, $p_b = 0.01$	2
	R. Isthmus cingulate cortex – R. Hippocampus *Augmented*, $r = 0.44$, $p_b = 6 \times 10^{-5}$	71
ADNI modified Preclinical Alzheimer's Cognitive Composite (PACC) *with Digit Symbol Substitution*	R. Entorhinal cortex – R. Hippocampus *Raw*, $r = 0.40$, $p_b = 0.001$	6
	R. Hippocampus – L. Rostral middle frontal cortex *Augmented*, $r = 0.44$, $p_b = 2 \times 10^{-5}$	161
ADNI modified Preclinical Alzheimer's Cognitive Composite (PACC) *with Trails B*	R. Parahippocampal cortex – R. Fusiform cortex *Raw*, $r = 0.41$, $p_b = 0.0005$	6
	R. Hippocampus – L. Rostral middle frontal cortex *Augmented*, $r = 0.44$, $p_b = 10^{-5}$	173
Everyday Cognition Study Partner Report (ECog SP) – *Memory*	L. Entorhinal cortex – L. Banks of superior temporal sulcus *Augmented*, $r = -0.37$, $p_b = 0.02$	1
Everyday Cognition Study Partner Report (ECog SP) – *Language*	L. Middle temporal cortex – L. Isthmus cingulate cortex *Augmented*, $r = -0.38$, $p_b = 0.01$	4
Everyday Cognition Study Partner Report (ECog SP) – *Plan*	R. Isthmus cingulate cortex – L. Inferior temporal cortex *Augmented*, $r = -0.39$, $p_b = 0.009$	2
Everyday Cognition Study Partner Report (ECog SP) – *Total*	L. Entorhinal cortex – L. Hippocampus *Raw*, $r = -0.37$, $p_b = 0.04$	1
	R. Isthmus cingulate cortex – L. Inferior temporal cortex *Augmented*, $r = -0.39$, $p_b = 0.006$	4
Logical Memory *Delayed Recall*	R. Hippocampus – L. Rostral middle frontal cortex *Augmented*, $r = 0.37$, $p_b = 0.01$	6
Trail Making Test, Part B *Time to complete*	R. Parahippocampal cortex – R. Fusiform cortex *Raw*, $r = -0.40$, $p_b = 0.001$	1
	R. Isthmus cingulate cortex – R. Hippocampus *Augmented*, $r = -0.37$, $p_b = 0.04$	1

Table 2: Significant correlations of non-MRI variables with brain connectivity in OASIS-3.

Non-MRI variable	Most correlated brain structural connection	# Sig. Conn
Age	L. Hippocampus – L. Thalamus *Raw*, r = -0.48, $p_b = 6 \times 10^{-36}$	362
	L. Hippocampus – R. Lingual cortex *Augmented*, r = -0.50, $p_b = 2 \times 10^{-42}$	2614
Age at entry	R. Hippocampus – R. Thalamus *Raw*, r = -0.47, $p_b = 7 \times 10^{-33}$	342
	R. Hippocampus – L. Superior frontal cortex *Augmented*, r = -0.49, $p_b = 2 \times 10^{-40}$	2720
Sex	L. Thalamus – R. Thalamus *Raw*, r = -0.21 (with the male sex), p_b = 0.001	1
Uniform Data Set (UDS)	L. Superior parietal cortex – L. Precuneus cortex *Raw*, r = 0.37, $p_b = 2 \times 10^{-19}$	109
	R. Inferior parietal cortex – L. Inferior parietal cortex *Augmented*, r = 0.34, $p_b = 10^{-14}$	2005
Neuropsychological Assessment	L. Superior parietal cortex – L. Precuneus cortex *Raw*, r = 0.38, $p_b = 4 \times 10^{-14}$	166
	L. Pericalcarine cortex – L. Parahippocampal cortex *Augmented*, r = 0.41, $p_b = 6 \times 10^{-18}$	2803
Mini-Mental State Examination (MMSE)	R. Hippocampus – R. Putamen *Raw*, r = 0.29, $p_b = 3 \times 10^{-10}$	61
	R. Hippocampus – L. Precentral cortex *Augmented*, r = 0.38, $p_b = 10^{-21}$	1066
Clinical Dementia Rating (CDR)	R. Amygdala – R. Hippocampus *Raw*, r = -0.33, $p_b = 7 \times 10^{-14}$	80
	R. Hippocampus – L. Thalamus *Augmented*, r = -0.41, $p_b = 3 \times 10^{-26}$	1616
Clinical Dementia Rating (CDR) *Community affairs*	R. Superior frontal cortex – R. Hippocampus *Augmented*, r = -0.35, $p_b = 8 \times 10^{-18}$	1009
Clinical Dementia Rating (CDR) *Home and hobbies*	R. Hippocampus – R. Amygdala *Raw*, r = -0.29, $p_b = 3 \times 10^{-10}$	55
	R. Hippocampus – L. Thalamus *Augmented*, r = -0.38, $p_b = 6 \times 10^{-22}$	1495
Clinical Dementia Rating (CDR) *Judgment and problem-solving*	R. Amygdala – R. Hippocampus *Raw*, r = -0.31, $p_b = 8 \times 10^{-12}$	71
	R. Superior frontal cortex – R. Hippocampus *Augmented*, r = -0.39, $p_b = 7 \times 10^{-23}$	1383
Clinical Dementia Rating (CDR) *Memory*	R. Amygdala – R. Hippocampus *Raw*, r = -0.34, $p_b = 4 \times 10^{-15}$	97
	R. Hippocampus – L. Thalamus *Augmented*, r = -0.41, $p_b = 10^{-26}$	1987
Clinical Dementia Rating (CDR) *Orientation*	R. Amygdala – R. Hippocampus *Raw*, r = -0.30, $p_b = 7 \times 10^{-11}$	57
	R. Hippocampus – L. Insula *Augmented*, r = -0.36, $p_b = 10^{-19}$	1533
Clinical Dementia Rating (CDR) *Personal Care*	R. Hippocampus – L. Thalamus *Augmented*, r = -0.19, p_b = 0.04	4

Clinical Dementia Rating (CDR) *Sum of boxes*	R. Hippocampus – R. Amygdala *Raw*, r = -0.32, $p_b = 7 \times 10^{-13}$	77
	R. Hippocampus – L. Thalamus *Augmented*, r = -0.40, $p_b = 7 \times 10^{-25}$	1698
Number of MRI Sessions	R. Middle temporal cortex – R. Hippocampus *Raw*, r = 0.35, $p_b = 10^{-16}$	125
	R. Precuneus cortex – R. Hippocampus *Augmented*, r = 0.38, $p_b = 5 \times 10^{-22}$	2346
Number of PET Sessions	R. Hippocampus – R. Fusiform cortex *Raw*, r = 0.3, $p_b = 10^{-8}$	44
	R. Cuneus cortex – L. Hippocampus *Augmented*, r = 0.34, $p_b = 3 \times 10^{-12}$	1008
Number of CT Sessions	R. Hippocampus – R. Fusiform cortex *Raw*, r = 0.23, p_b = 0.03	1
	R. Superior frontal cortex – R. Hippocampus *Augmented*, r = 0.25, p_b = 0.0004	2
ADRC Clinical Data	L. Superior parietal cortex – L. Precuneus cortex *Raw*, r = 0.31, $p_b = 2 \times 10^{-12}$	97
	R. Inferior parietal cortex – R. Fusiform cortex *Augmented*, r = 0.31, $p_b = 9 \times 10^{-13}$	1608

Table 3: Significant correlations of non-MRI variables with brain connectivity in PREVENT-AD.

Non-MRI variable	Most correlated brain structural connection	# Sig. Conn
Age	R. Hippocampus – R. Thalamus *Raw*, r = -0.33, p_b = 0.002	2
	L. Hippocampus – R. Thalamus *Augmented*, r = -0.33, p_b = 0.001	13
Age of mother at AD-like dementia onset	R. Ventral diencephalon – L. Banks of superior temporal sulcus *Raw*, r = -0.36, p_b = 0.006	1
Tau phosphorylated at Thr181 (P-tau) concentration in CSF	R. Caudate – L. Caudal middle frontal cortex *Raw*, r = 0.45, p_b = 0.04	1

Table 4: Significant correlations of non-MRI variables with brain connectivity in HCP.

Non-MRI variable	Most correlated brain structural connection	# Sig. Conn
Height	Brainstem – L. Lingual cortex *Raw*, r = -0.25, p_b = 0.02	1
Weight	R. Ventral diencephalon – L. Ventral diencephalon *Raw*, r = -0.26, p_b = 0.006	1

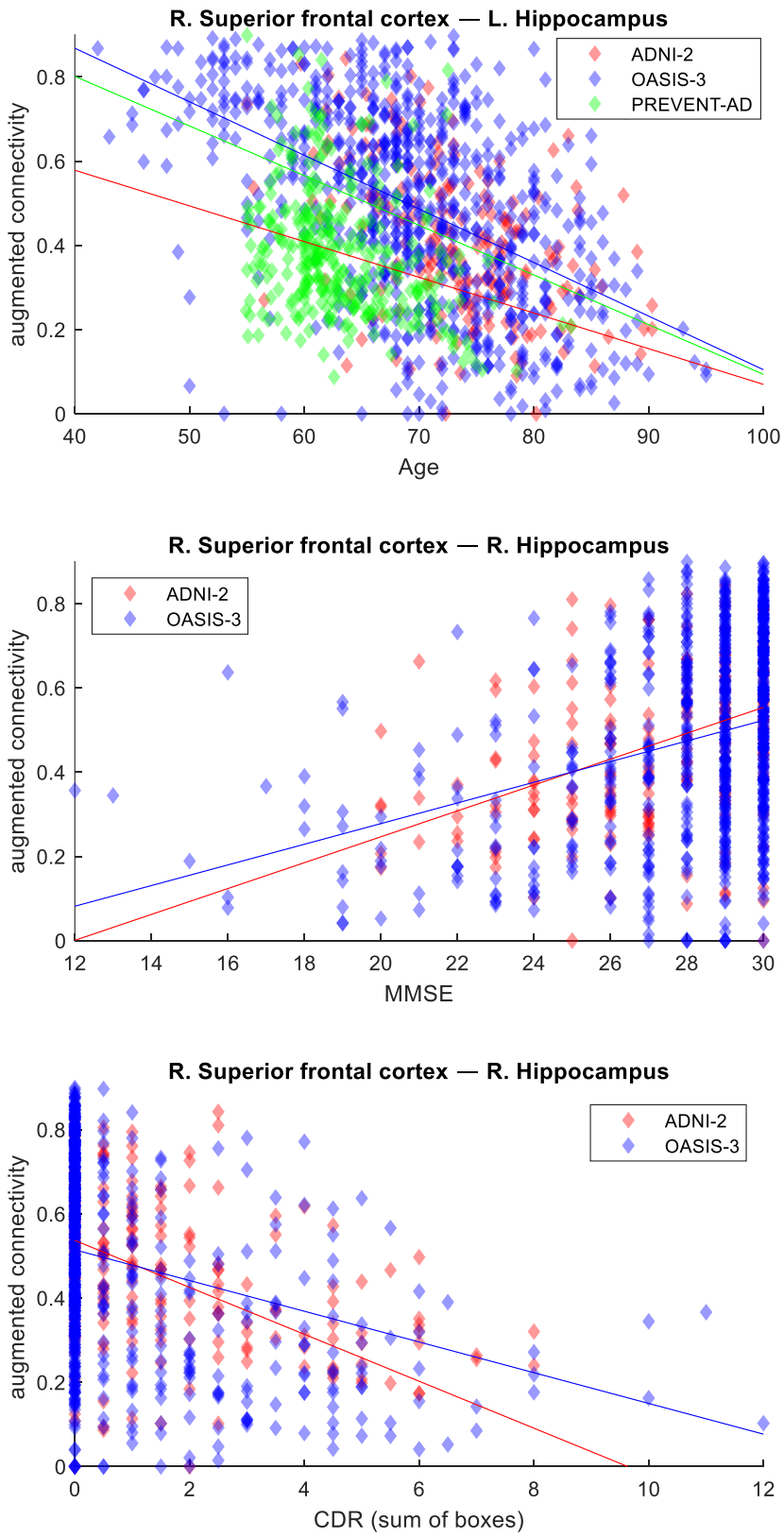

Figure 1. Augmented connectivity of the brain connection most significantly correlated with age (top), MMSE (middle), and CDR (bottom) consistently across databases.

4. Discussion

Although more correlations were initially found to be significant with raw than augmented structural connectivity (in three out of four databases), visual inspection of the data led to discarding many of the former – but none of the latter – as spurious, implying more robustness and reliability of the augmented structural connections. Spuriousness was often because raw (direct) connectivity between an ROI pair was zero for all except a few subjects that dramatically influenced the correlation calculation, in contrast to augmented connectivity that is always positive in a network with a single connected component. Eventually, a total of 36 relationships with raw connectivity and 38 with augmented connectivity passed the Pearson correlation threshold, Bonferroni correction, and visual inspection. Each variable may have been significantly correlated with multiple brain connections, the number of which is listed in the tables (right column). Out of 30 variables correlated with both types of connectivity, 28 were more significantly correlated with augmented than raw connectivity, always with a greater or equal number of total connections correlated with augmented than raw connectivity. For a significance plot of the correlation with age, MMSE, and CDR for all connections (albeit in a non-exploratory context and with a different connectivity quantification method), see our previous report [18].

More variables were found to be significantly related to brain connectivity in ADNI-2 and OASIS-3 than in PREVENT-AD and HCP, possibly due to many more variables that were tested in the latter databases (hence more aggressive correction for multiple comparisons). Another potential reason may be that PREVENT-AD and HCP (that include only healthy subjects) are more homogenous populations with narrower ranges of disease-severity scores (e.g. MMSE) than ADNI-2 and OASIS-3 (that include a mix of healthy, MCI, and AD subjects).

The most prominent non-MRI variable that was consistently correlated with structural connectivity was age. A negative correlation was observed between age and hippocampal connectivity in all databases except HCP. The limited age range in the young population of HCP may be the reason why this relationship was not detected in this database, given that the standard deviations of age were (in decreasing order) 9.1 years in OASIS-3, 6.9 years in ADNI-2, 5.1 years in PREVENT-AD, but only 3.6 years in HCP. In fact, the statistical significance of the age correlation decreased in the same database order.

Clinical scores that were found to be significantly related to brain connectivity showed the consistent trend of healthier score being linked to increased connectivity. The only exception was the significant relationship of P-tau with the raw connection between the right caudate and the left caudal middle frontal cortex in PREVENT-AD, which was unanticipatedly *positive*. Nonetheless, we had already observed – in a different database with a different connectivity quantification method – a similarly unexpected strengthening of caudal structural connectivity with worsening cognitive status [18, 37]. In fact, volume [38] and fractional anisotropy (FA) [39] of the caudate have been reported to increase in pre-symptomatic familial AD, which might have also led to the aforementioned relationship we observed in PREVENT-AD (that includes healthy subjects at risk

of AD). Such an increase in the measured structural connectivity in pre-symptomatic subjects may indicate a compensatory effect [40], or could stem from other factors (e.g., selective axonal loss can increase FA in regions with fiber crossing [39, 41, 42]).

The number of imaging sessions and data available for a subject in OASIS-3 was positively related to (mostly) hippocampal connectivity. This could be attributable to a higher follow-up rate for those with healthier hippocampi, as individuals with MCI and dementia have been shown to have lower retention rates in research studies than those with normal cognition [43, 44].

With larger ICV, brain regions become farther apart from each other, thus harder to reach by streamline tractography. Therefore, we decided to control for ICV in our regression analysis to avoid underestimation of brain connectivity. Doing so eliminated (in some databases) possibly spurious correlation of brain connectivity with variables that might be correlated with ICV, i.e., strength, sex, and alcohol consumption. Correlation of brain connectivity with sex [45], in particular, remained inconclusive, given that it disappeared after ICV adjustment in PREVENT-AD and HCP, as is typically seen in neuroimaging studies [46, 47], and appeared in ADNI-2 only after ICV adjustment, which could be a sign of an introduced (previously absent) ICV bias [48] (especially as the direction of the relationship was opposite to that in OASIS-3).

To correct for multiple comparisons, we took the conservative Bonferroni approach to avoid false-positive relationships with brain connectivity (reduce type I errors). Strong interdependencies both between brain connections and between non-MRI variables can nevertheless be exploited to design a complex but more forgiving correction scheme in order to avoid false negatives and missing existing relationships (reduce type II errors).

5. Conclusions

We conducted a retrospective exploratory study to examine the associations between brain structural connectivity and non-MRI variables, using data from four (including three AD-related) public dMRI databases. Unlike hypothesis-driven research, where conjectured relationships between specific variables are tested, we calculated the correlation between all brain connections and non-MRI variables in our dataset without prior assumption, while stringently correcting for multiple comparisons, with the aim of discovering connectomic relationships. Replication of our findings in other databases and with other connectivity quantification methods is a subject of future research.

Acknowledgements

Support for this research was provided by the National Institutes of Health (NIH), specifically the National Institute on Aging (NIA; R56AG068261, RF1AG068261).

Additional support was provided in part by the BRAIN Initiative Cell Census/Atlas Network grants U01MH117023 and UM1MH130981, the National Institute for Biomedical Imaging and Bioengineering (NIBIB; P41EB015896, R01EB023281, R01EB006758, R21EB018907, R01EB019956, P41EB030006), the NIA (R21AG082082, R56AG064027, R01AG064027, R01AG008122, R01AG016495, R01AG070988), the National Institute of Mental Health (R01MH121885, RF1MH123195), the National Institute for Neurological Disorders and Stroke (R01NS0525851, R21NS072652, R01NS070963, R01NS083534, U01NS086625, U24NS10059103, R01NS105820), the NIH Blueprint for Neuroscience Research (U01MH093765), part of the multi-institutional Human Connectome Project, the BrightFocus Foundation (A2016172S), and the Michael J. Fox Foundation for Parkinson's Research (MJFF-021226).

Computational resources were provided through the Massachusetts Life Sciences Center and NIH Shared Instrumentation Grants (S10RR023401, S10RR019307, S10RR023043, S10RR028832).

Data collection and sharing for this project was funded in part by the Alzheimer's Disease Neuroimaging Initiative (ADNI) (NIH Grant U01 AG024904) and DOD ADNI (Department of Defense award number W81XWH-12-2-0012). ADNI is funded by the NIA, the NIBIB, and through generous contributions from the following: AbbVie, Alzheimer's Association; Alzheimer's Drug Discovery Foundation; Araclon Biotech; BioClinica, Inc.; Biogen; Bristol-Myers Squibb Company; CereSpir, Inc.; Cogstate; Eisai Inc.; Elan Pharmaceuticals, Inc.; Eli Lilly and Company; EuroImmun; F. Hoffmann-La Roche Ltd and its affiliated company Genentech, Inc.; Fujirebio; GE Healthcare; IXICO Ltd.; Janssen Alzheimer Immunotherapy Research & Development, LLC.; Johnson & Johnson Pharmaceutical Research & Development LLC.; Lumosity; Lundbeck; Merck & Co., Inc.; Meso Scale Diagnostics, LLC.; NeuroRx Research; Neurotrack Technologies; Novartis Pharmaceuticals Corporation; Pfizer Inc.; Piramal Imaging; Servier; Takeda Pharmaceutical Company; and Transition Therapeutics. The Canadian Institutes of Health Research is providing funds to support ADNI clinical sites in Canada. Private sector contributions are facilitated by the Foundation for the National Institutes of Health (www.fnih.org). The grantee organization is the Northern California Institute for Research and Education, and the study is coordinated by the Alzheimer's Therapeutic Research Institute at the University of Southern California. ADNI data are disseminated by the Laboratory for Neuro Imaging at the University of Southern California.

Data were also provided in part by OASIS-3: Longitudinal Multimodal Neuroimaging: Principal Investigators: T. Benzinger, D. Marcus, J. Morris; NIH P30 AG066444, P50 AG00561, P30 NS09857781, P01 AG026276, P01 AG003991, R01 AG043434, UL1 TR000448, R01 EB009352. AV-45 doses were provided by Avid Radiopharmaceuticals, a wholly owned subsidiary of Eli Lilly.

Data were also obtained in part from the Pre-symptomatic Evaluation of Novel or Experimental Treatments for Alzheimer's Disease (PREVENT-AD) program.

Data were furthermore provided in part by the Human Connectome Project (HCP), WU-Minn Consortium (Principal Investigators: David Van Essen and Kamil Ugurbil; 1U54MH091657) funded by the 16 NIH Institutes and Centers that support the NIH Blueprint for Neuroscience Research; and by the McDonnell Center for Systems Neuroscience at Washington University.

B. Fischl has a financial interest in CorticoMetrics, a company whose medical pursuits focus on brain imaging and measurement technologies. His interests were reviewed and are managed by Massachusetts General Hospital and Mass General Brigham in accordance with their conflict-of-interest policies.

References

[1] Tijms BM, Wink AM, de Haan W, van der Flier WM, Stam CJ, Scheltens P, et al. Alzheimer's disease: connecting findings from graph theoretical studies of brain networks. Neurobiology of Aging. 2013;34:2023-36.

[2] Filippi M, Agosta F. Structural and functional network connectivity breakdown in Alzheimer's disease studied with magnetic resonance imaging techniques. Journal of Alzheimer's Disease. 2011;24:455-74.

[3] de LaCoste M-C, White CL. The role of cortical connectivity in Alzheimer's disease pathogenesis: A review and model system. Neurobiology of Aging. 1993;14:1-16.

[4] Sporns O. The human connectome: a complex network. Annals of the New York Academy of Sciences. 2011;1224:109-25.

[5] Hafkemeijer A, van der Grond J, Rombouts SARB. Imaging the default mode network in aging and dementia. Biochimica et Biophysica Acta (BBA) - Molecular Basis of Disease. 2012;1822:431-41.

[6] Greicius MD, Srivastava G, Reiss AL, Menon V. Default-mode network activity distinguishes Alzheimer's disease from healthy aging: Evidence from functional MRI. Proceedings of the National Academy of Sciences of the United States of America. 2004;101:4637-42.

[7] Lee WJ, Han CE, Aganj I, Seo SW, Seong J-K. Distinct Patterns of Rich Club Organization in Alzheimer’s Disease and Subcortical Vascular Dementia: A White Matter Network Study. Journal of Alzheimer's Disease. 2018;63:977-87.

[8] Rose SE, Chen F, Chalk JB, Zelaya FO, Strugnell WE, Benson M, et al. Loss of connectivity in Alzheimer's disease: an evaluation of white matter tract integrity with colour coded MR diffusion tensor imaging. Journal of Neurology, Neurosurgery & Psychiatry. 2000;69:528-30.

[9] Chhatwal JP, Schultz AP, Johnson KA, Hedden T, Jaimes S, Benzinger TLS, et al. Preferential degradation of cognitive networks differentiates Alzheimer’s disease from ageing. Brain. 2018;141:1486-500.

[10] Rubinov M, Sporns O. Complex network measures of brain connectivity: Uses and interpretations. NeuroImage. 2010;52:1059-69.

[11] Reijmer YD, Leemans A, Caeyenberghs K, Heringa SM, Koek HL, Biessels GJ, et al. Disruption of cerebral networks and cognitive impairment in Alzheimer disease. Neurology. 2013;80:1370-7.

[12] Jbabdi S, Johansen-Berg H. Tractography: Where do we go from here? Brain Connectivity. 2011;1:169-83.

[13] Aganj I, Lenglet C, Jahanshad N, Yacoub E, Harel N, Thompson PM, et al. A Hough transform global probabilistic approach to multiple-subject diffusion MRI tractography. Med Image Anal. 2011;15:414-25.

[14] Honey CJ, Sporns O, Cammoun L, Gigandet X, Thiran JP, Meuli R, et al. Predicting human resting-state functional connectivity from structural connectivity. Proceedings of the National Academy of Sciences. 2009;106:2035-40.

[15] Deligianni F, Robinson E, Beckmann CF, Sharp D, Edwards AD, Rueckert D. Inference of functional connectivity from direct and indirect structural brain connections. Biomedical Imaging: From Nano to Macro, 2011 IEEE International Symposium on2011. p. 849-52.

[16] Aganj I, Prasad G, Srinivasan P, Yendiki A, Thompson PM, Fischl B. Structural brain network augmentation via Kirchhoff's laws. Annual Meeting of the International Society for Magnetic Resonance in Medicine2014.

[17] Frau-Pascual A, Fogarty M, Fischl B, Yendiki A, Aganj I. Quantification of structural brain connectivity via a conductance model. NeuroImage. 2019;189:485-96.

[18] Frau-Pascual A, Augustinack J, Varadarajan D, Yendiki A, Salat DH, Fischl B, et al. Conductance-Based Structural Brain Connectivity in Aging and Dementia. Brain Connectivity. 2021;11:566-83.

[19] Wyman BT, Harvey DJ, Crawford K, Bernstein MA, Carmichael O, Cole PE, et al. Standardization of analysis sets for reporting results from ADNI MRI data. Alzheimer's & Dementia: The Journal of the Alzheimer's Association. 2013;9:332-7.

[20] LaMontagne PJ, Keefe S, Lauren W, Xiong C, Grant EA, Moulder KL, et al. P3-083: OASIS-3: Longitudinal neuroimaging, clinical, and cognitive dataset for normal aging and Alzheimer's disease. Alzheimer's & Dementia. 2018;14:P1097-P.

[21] Tremblay-Mercier J, Madjar C, Das S, Pichet Binette A, Dyke SOM, Étienne P, et al. Open science datasets from PREVENT-AD, a longitudinal cohort of pre-symptomatic Alzheimer's disease. NeuroImage: Clinical. 2021;31:102733.

[22] Van Essen DC, Smith SM, Barch DM, Behrens TEJ, Yacoub E, Ugurbil K. The WU-Minn Human Connectome Project: An overview. NeuroImage. 2013;80:62-79.

[23] Fischl B. FreeSurfer. NeuroImage. 2012;62:774-81.

[24] Reuter M, Schmansky NJ, Rosas HD, Fischl B. Within-subject template estimation for unbiased longitudinal image analysis. NeuroImage. 2012;61:1402-18.

[25] Jenkinson M, Beckmann CF, Behrens TEJ, Woolrich MW, Smith SM. FSL. NeuroImage. 2012;62:782-90.

[26] Greve DN, Fischl B. Accurate and robust brain image alignment using boundary-based registration. NeuroImage. 2009;48:63-72.

[27] Aganj I, Lenglet C, Sapiro G, Yacoub E, Ugurbil K, Harel N. Reconstruction of the orientation distribution function in single- and multiple-shell q-ball imaging within constant solid angle. Magnetic Resonance in Medicine. 2010;64:554-66.

[28] Greicius MD, Supekar K, Menon V, Dougherty RF. Resting-State Functional Connectivity Reflects Structural Connectivity in the Default Mode Network. Cerebral Cortex. 2008;19:72-8.

[29] Adachi Y, Osada T, Sporns O, Watanabe T, Matsui T, Miyamoto K, et al. Functional Connectivity between Anatomically Unconnected Areas Is Shaped by Collective Network-Level Effects in the Macaque Cortex. Cerebral Cortex. 2011;22:1586-92.

[30] Damoiseaux J, Greicius M. Greater than the sum of its parts: a review of studies combining structural connectivity and resting-state functional connectivity. Brain Struct Funct. 2009;213:525-33.

[31] Huang H, Ding M. Linking Functional Connectivity and Structural Connectivity Quantitatively: A Comparison of Methods. Brain Connectivity. 2016;6:99-108.

[32] Koch MA, Norris DG, Hund-Georgiadis M. An Investigation of Functional and Anatomical Connectivity Using Magnetic Resonance Imaging. NeuroImage. 2002;16:241-50.

[33] Skudlarski P, Jagannathan K, Calhoun VD, Hampson M, Skudlarska BA, Pearlson G. Measuring brain connectivity: Diffusion tensor imaging validates resting state temporal correlations. NeuroImage. 2008;43:554-61.

[34] van den Heuvel MP, Mandl RCW, Kahn RS, Hulshoff Pol HE. Functionally linked resting-state networks reflect the underlying structural connectivity architecture of the human brain. Human Brain Mapping. 2009;30:3127-41.

[35] Chung MK, Hanson JL, Adluru N, Alexander AL, Davidson RJ, Pollak SD. Integrative Structural Brain Network Analysis in Diffusion Tensor Imaging. Brain Connectivity. 2017;7:331-46.

[36] Rousselet G, Pernet C. Improving standards in brain-behavior correlation analyses. Frontiers in Human Neuroscience. 2012;6.

[37] Aganj I, Frau-Pascual A, Iglesias JE, Yendiki A, Augustinack JC, Salat DH, et al. Compensatory brain connection discovery in Alzheimer's disease. 2020 IEEE 17th International Symposium on Biomedical Imaging (ISBI) 2020. p. 283-7.

[38] Fortea J, Sala-Llonch R, Bartrés-Faz D, Bosch B, Lladó A, Bargalló N, et al. Increased cortical thickness and caudate volume precede atrophy in PSEN1 mutation carriers. Journal of Alzheimer's Disease. 2010;22:909-22.

[39] Ryan NS, Keihaninejad S, Shakespeare TJ, Lehmann M, Crutch SJ, Malone IB, et al. Magnetic resonance imaging evidence for presymptomatic change in thalamus and caudate in familial Alzheimer’s disease. Brain. 2013;136:1399-414.

[40] Stern Y. Cognitive Reserve and Alzheimer Disease. Alzheimer Disease & Associated Disorders. 2006;20:S69-S74.

[41] Douaud G, Jbabdi S, Behrens TEJ, Menke RA, Gass A, Monsch AU, et al. DTI measures in crossing-fibre areas: Increased diffusion anisotropy reveals early white matter alteration in MCI and mild Alzheimer's disease. NeuroImage. 2011;55:880-90.

[42] Kim WH, Adluru N, Chung MK, Okonkwo OC, Johnson SC, B. Bendlin B, et al. Multi-resolution statistical analysis of brain connectivity graphs in preclinical Alzheimer's disease. NeuroImage. 2015;118:103-17.

[43] Grill JD, Kwon J, Teylan MA, Pierce A, Vidoni ED, Burns JM, et al. Retention of Alzheimer Disease Research Participants. Alzheimer Disease & Associated Disorders. 2019;33:299-306.

[44] Lo RY, Jagust WJ. Predicting missing biomarker data in a longitudinal study of Alzheimer disease. Neurology. 2012;78:1376-82.

[45] Jahanshad N, Aganj I, Lenglet C, Joshi A, Yan J, Barysheva M, et al. Sex differences in the human connectome: 4-Tesla high angular resolution diffusion imaging (HARDI) tractography in 234 young adult twins. Biomedical Imaging: From Nano to Macro, 2011 IEEE International Symposium on 2011. p. 939-43.

[46] Leonard CM, Towler S, Welcome S, Halderman LK, Otto R, Eckert MA, et al. Size Matters: Cerebral Volume Influences Sex Differences in Neuroanatomy. Cerebral Cortex. 2008;18:2920-31.

[47] Choi C-H, Lee J-M, Koo B-B, Park JS, Kim D-S, Kwon JS, et al. Sex differences in the temporal lobe white matter and the corpus callosum: a diffusion tensor tractography study. NeuroReport. 2010;21:73-7.

[48] Dhamala E, Ooi LQR, Chen J, Kong R, Anderson KM, Chin R, et al. Proportional intracranial volume correction differentially biases behavioral predictions across neuroanatomical features, sexes, and development. NeuroImage. 2022;260:119485.